# Performance Optimization of a High Current Dual Active Bridge with a Wide Operating Voltage Range

**F. Krismer, S. Round, J. W. Kolar**
ETH Zurich, Power Electronic Systems Laboratory
ETL I16, Physikstrasse 3
CH-8092 Zurich, SWITZERLAND
krismer@lem.ee.ethz.ch round@lem.ee.ethz.ch kolar@lem.ee.ethz.ch

***Abstract* — The main aim of this paper is to improve the performance of high current dual active bridge converters when operated over a wide voltage range. A typical application is for fuel cell vehicles where a bi-directional interface between a 12V battery and a high voltage DC bus is required. The battery side voltage ranges from 11V to 16V while the fuel cell is operated between 220V and 447V and the required power is typically 1kW. Careful analysis shows that the high currents on the battery side cause significant design issues in order to obtain a high efficiency. The standard phase shift modulation method can result in high conduction and switching losses. This paper proposes a combined triangular and trapezoidal modulation method to reduce losses over the wide operating range. Approximately, a 2% improvement in efficiency can be expected. An experimental system is used to verify the improved performance of the dual active bridge using the proposed advanced modulation method.**

## I. INTRODUCTION

A dual active bridge (DAB) converter with high power density and soft switching operation is proposed as a bi-directional DC to DC interface to convert electric energy between a low voltage battery and a high voltage DC bus. A typical application is in fuel-cell powered electric vehicles where a battery is used to provide the high DC voltage during start-up. Under normal operation this converter is used in the reverse direction to charge the battery from the high voltage DC bus as well as to supply power to 12V auxiliary loads [1].

The required input and output voltage ranges of the bi-directional DC/DC converter for a typical automotive application are presented in **Figure 1**. The battery side voltage ($V_1$) ranges from 11V to 16V and the fuel cell output voltage ($V_2$) is between 220V and 447V. The required maximum output power is 1kW over the specified voltage range and results in a large DC current of up to 100A on the low voltage side. This high current produces significant challenges in designing a compact and efficient converter.

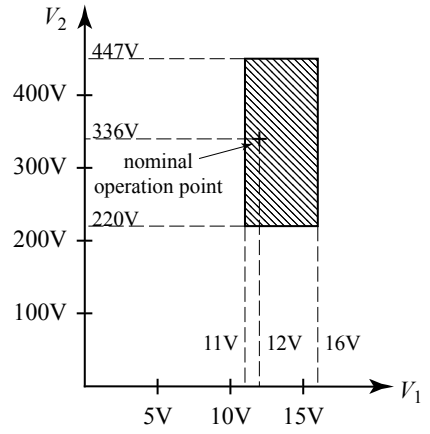


**Figure 1.** Converter operating voltage ranges required for automotive application.

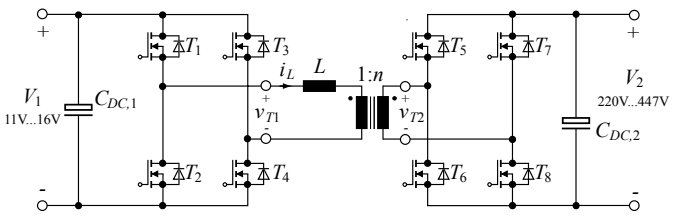


**Figure 2.** Dual active bridge (DAB) converter.

The dual active bridge topology (**Figure 2**, [2]) is selected for this application because it has the attractive feature of a low number of components when compared to other bidirectional DC/DC converters such as those presented in [3] and [4]. The power flow of the DAB is typically controlled with phase shift modulation. However, it is shown in this paper, that the performance of the DAB can be improved with an alternative modulation method.

In this paper the difficulties associated with the switching of high transistor currents are described in **Section II** using a simplified MOSFET model. The consequences of operating the DAB with standard phase-shift modulation are evaluated with simulation in **Section III**. An alternative modulation

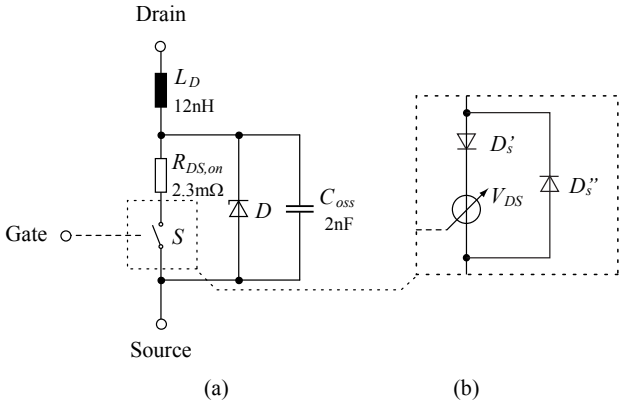


**Figure 3.** Transistor model to simulate switching losses at high transistor currents.

method is investigated in order to increase the performance of the converter. In **Section IV** experimental results are presented in order to verify the performance of the modulation schemes. The aim of the paper is to show that the performance of a high current DAB is improved with the use of an alternative modulation method.

## II. HIGH CURRENT MOSFET SWITCHING MODEL

For the specified application, the low voltage side transformer current ($i_L$ in **Figure 2**) reaches RMS values of more than 100A and the transistor current during switching can be even higher. In order to compare the different modulation methods, the switching losses need to be determined as a function of transistor voltage and current. Therefore, the influence of a high transistor current during switching is investigated for a half bridge arrangement using on a simplified transistor model (**Figure 3**). The transistor model is derived from models presented in [6] and [7]. It consists of a switch $S$, a series resistance $R_{DS,on}$, a parallel capacitor $C_{oss}$ for the junction capacitance and a zener diode $D$, which models the body diode and the breakdown behaviour of the MOSFET. The series inductor $L_D$ models the parasitic inductance of bond wires and connecting terminals. The component values given in Figure 3 are based on datasheet values for the IRF2804 MOSFET, that is

- $V_{(BR)DSS}$ = 40V,
- $I_{D,\max}$ = 75A,
- $R_{DS,on}$ = 2.3mΩ.

These values are used for all subsequent calculations and simulations. Limited rise and fall times of the switch voltage is accounted for in simulation. There the switch has been replaced with a voltage source $V_{DS}$ connected in series to an ideal diode $D_S'$ (Figure 3 (b)). The ideal diode $D_S''$ is used to model synchronous rectification.

Simulation and experimental verification of the switching losses are carried out for a half bridge converter when operated with zero voltage switching (ZVS). As zero voltage turn-on of $T_1$ is achieved, it is sufficient to only consider the turn-off losses.

If the non-ideal dynamic behaviour of the switch $S$ is neglected and only the influence of the parasitic inductor $L_D$ is considered, then the energy $E_{off}$ that is dissipated can be calculated by evaluating

$$E_{off} = \frac{1}{2} \cdot \left(L_{D,1} + L_{D,2}\right) \cdot I_D^2 \cdot \frac{V_{(BR)DSS}}{V_{(BR)DSS} - V_1} \qquad (1)$$

where $L_{D,1}$ and $L_{D,2}$ are the parasitic inductances of the switches, $I_D$ is the switching current, $V_1$ is the supply voltage of the half bridge and $V_{(BR)DSS}$ is the breakdown voltage of the MOSFET. This yields a good approximation of the switching losses for high device currents ($I_D$ > 100A).

In **Figure 4** the theoretically calculated switching losses (based on (1)) are compared to the simulated and the measured values. The result reflects a good match for high currents while for low currents an error exists due to the simplified model. This result shows that significant switching losses occur for high currents. Equation (1) suggests a

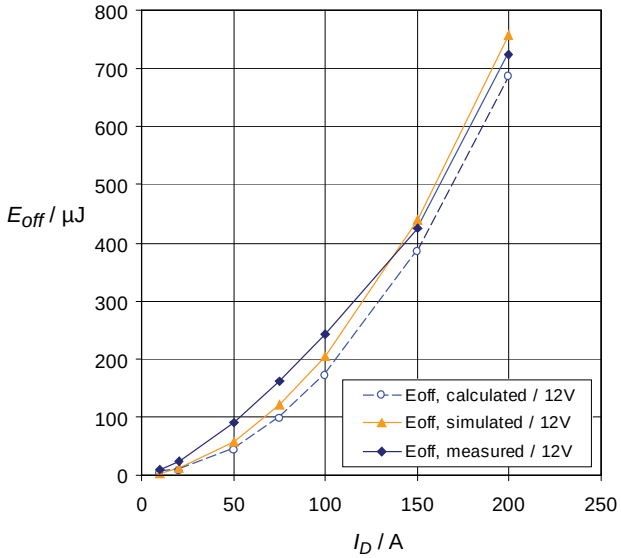


**Figure 4.** Calculated and measured turn-off losses for the IRF2804S MOSFET ($V_1$=12V, $T$=25°C).

reduction of the parasitic inductances $L_{D,1}$ and $L_{D,2}$ in order to reduce switching losses, which can be achieved by using MOSFETs in parallel. Also, a modulation method is proposed, which allows for zero current switching (ZCS) on the low voltage side of the converter.

## III. MODULATION METHODS FOR HIGH CURRENT DUAL ACTIVE BRIDGES

This section considers different modulation methods for the DAB as well as the influence on converter efficiency. Firstly, phase shift modulation is characterized, because it is the most common modulation method to operate the DAB. Then alternative modulation methods, triangular and trapezoidal, are presented in order to provide better converter performance.

For the design calculations of the converter, a switching frequency $f_S$ of 100kHz and an efficiency of 85% (at $V_1$ = 11V, $V_2$=220V) is assumed.

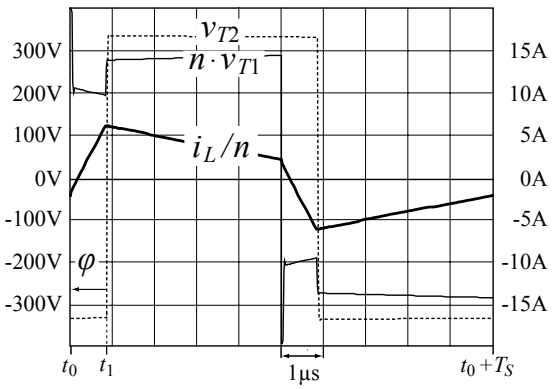


**Figure 5.** Simulated waveforms for the converter current and converter voltages for phase shift operation ($V_1$ = 12V, $V_2$ = 336V, output power: 1kW, $f_S$ = 100kHz).

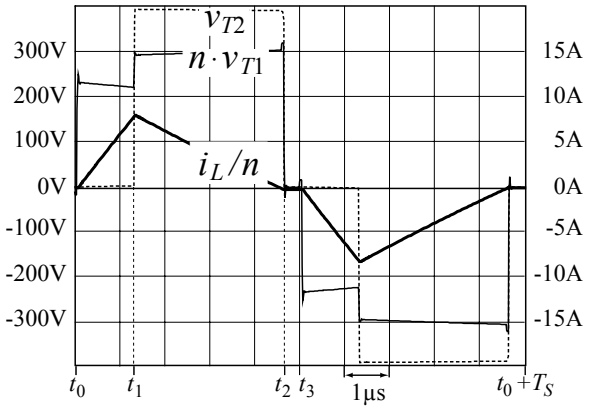


**Figure 6.** Simulated waveforms for the triangular current mode modulation at $V_1$ = 12V and $V_2$ = 400V and an output power of 1kW, transferred from the low voltage to the high voltage side.

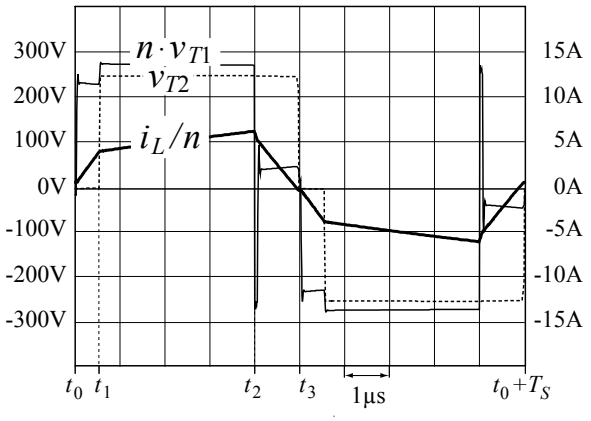


**Figure 7.** Simulated waveforms for the trapezoidal current mode modulation at $V_1$ = 12V and $V_2$ = 250V and an output power of 1kW, transferred from the low voltage to the high voltage side.

*A. Phase shift operation*

For phase shift operation, rectangular transformer voltages $v_{T1}(t)$ and $v_{T2}(t)$ with switching frequency $f_S$ and phase shift $\varphi$ are applied to the transformer and the converter inductance $L$ (**Figure 5**, [2]). The phase shift angle $\varphi$ controls the transferred power,

$$P = \frac{V_1 V_2 / n \cdot \varphi \cdot (\pi - \varphi)}{2\pi^2 f_S L}. \qquad (2)$$

This equation can be used to design the inductance $L$ of the DAB. For a transformer turns ratio of $n$ = 24, an inductor value of $L$ = 95 nH is calculated. These component values are used for all further analysis of the DAB operated with phase shift modulation.

The simplicity of the phase shift method and the possibility of using half bridge circuits to generate the high frequency transformer voltages $v_{T1}(t)$ and $v_{T2}(t)$ are the main reasons for the wide use of this modulation method. However, a high level of reactive power circulates in the high frequency transformer when the operating point is significantly different to the nominal operating point. For phase shift modulation it is not possible to directly influence the shape of the transformer current since it depends on the DC voltages $V_1$ and $V_2$ as well as on the phase shift $\varphi$ (assuming a constant switching frequency $f_S$).

*B. Triangular current mode modulation*

The disadvantages of phase shift modulation give reason to investigate alternative modulation methods. With the use of two full bridges (Figure 2) it is possible to generate three level transformer voltages $v_{T1}(t)$ and $v_{T2}(t)$ with an arbitrary duty cycle. This enables modulation principles different to the phase shift modulation, giving a reduction of the transformer reactive power and a reduction of switching losses. In this context, two different modulation methods are described: the triangular and the trapezoidal modulation methods. Triangular modulation is used when the voltages $V_1$ and $V_2/n$ are significantly different [5]. The modulation results in a transformer current that can be divided into three different time segments (**Figure 6**). During the first time segment ($t_0 < t < t_1$) the transformer current increases from zero. Subsequently the current reduces back to zero during the second time segment ($t_1 < t < t_2$). The transformer current is zero during the third time segment ($t_2 < t < t_3$) which is used to keep the switching frequency constant.

This method allows for the implementation of ZCS for the low voltage side, which is desired for low switching losses, high switching speed, and low EMI. This modulation method can be implemented when the transformer has a turns ratio such that $V_1 \ll V_2/n$. In this method the parasitic inductors of the low voltage side switches are utilized as part of the converter inductance $L$. It is particularly interesting for the specific converter because of the low value of $L$.

*C. Trapezoidal modulation*

Even though the triangular current mode modulation is a good choice for low switching losses, it comes with the disadvantage that the condition $V_1 \ll V_2/n$ needs to be fulfilled for the whole range of given input and output voltages $V_1$ and $V_2$. This in turn leads to ineffective converter utilization. If pure ZCS is not mandatory on the low voltage side, then the trapezoidal modulation can be used (**Figure 7**) as it is applicable for the condition of $V_1 \approx V_2/n$ [5]. Three different time segments in the transformer current can be distinguished. The first segment ($t_0 < t < t_1$) is, where the transformer current increases from zero. During the second segment ($t_1 < t < t_2$) the input and output voltages are applied to the transformer and in the final segment ($t_2 < t < t_3$) the transformer current decreases back to zero.

With trapezoidal modulation good converter efficiency is achieved. This is because the full bridge circuits are operating with large duty cycles and results in a lower RMS current than for triangular modulation. ZCS occurs for four transistors and ZVS for the remaining four, therefore reduced switching losses are expected compared to phase shift modulation.

*D. Full range operation*

The triangular and trapezoidal methods need to be combined in order to utilize the advanced modulation over

the full operating range. The choice of modulation scheme depends on the power level and the voltages $V_1$ and $V_2$. For a transformer turns ratio of $n = 24$ the power level where the transition between the two modulation schemes occurs is depicted in **Figure 8**. It is defined from [5] as

$$P_{\Delta} = \frac{V_1^2 \cdot (V_2/n - V_1)}{4 f_S L V_2/n} \quad \text{f. } V_1 \le V_2/n\,, \tag{3}$$

$$P_{\Delta} = \frac{V_2^2/n^2 \cdot (V_1 - V_2/n)}{4 f_S L V_1} \quad \text{f. } V_1 \ge V_2/n\,. \tag{4}$$

The shaded area in Figure 8 marks the region where the converter is operated with trapezoidal transformer current for a power level of 1kW. The modulation transitions to the triangular modulation method outside this shaded area. The figure also shows that the area, in which trapezoidal modulation is used, decreases for a power level of 500W while the area increases for 1500W. The maximum power that can be transferred with the combined modulation scheme is defined from [5] as

$$P_{\max} = \frac{V_1^2 V_2^2/n^2}{4 f_S L \cdot \left(V_1^2 + V_1 V_2/n + V_2^2/n^2\right)}. \tag{5}$$

Based on this equation the design for the DAB results in a calculated inductance of $L = 70$nH.

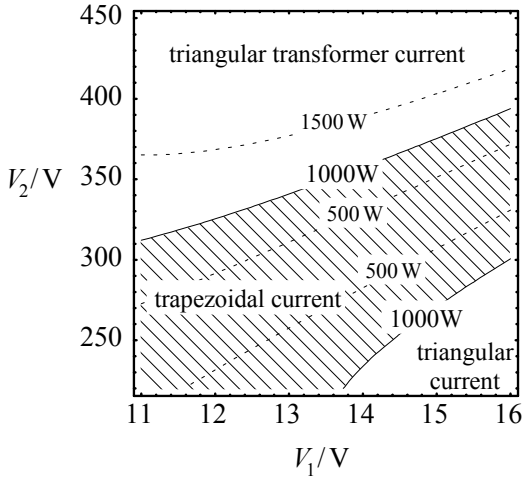


**Figure 8.** Illustrates the boundary between the trapezoidal and the triangular modulation methods for varying power levels.

*E. Comparison of the modulation methods*

The standard phase shift modulation method is simple to implement since the power flow can be directly controlled with the phase angle $\varphi$ by evaluating (2). It is sufficient to

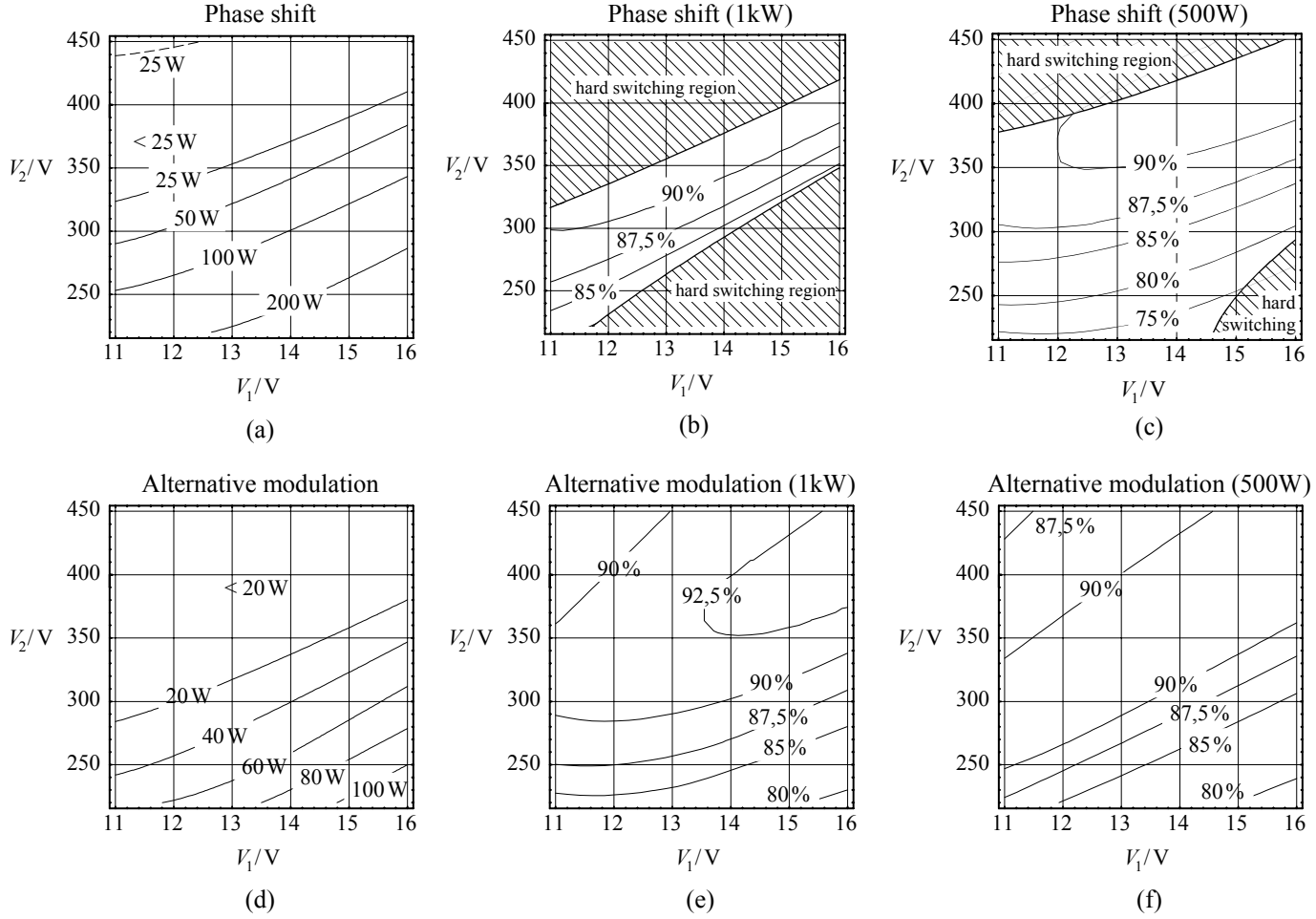


**Figure 9.** Calculated switching losses on the low voltage side and calculated efficiencies for phase shift modulation ((a) to (c)) and combined trapezoidal and triangular current mode modulation ((d) to (e)). Output power levels: 1kW ((b), (e)) and 500W ((c), (f)).

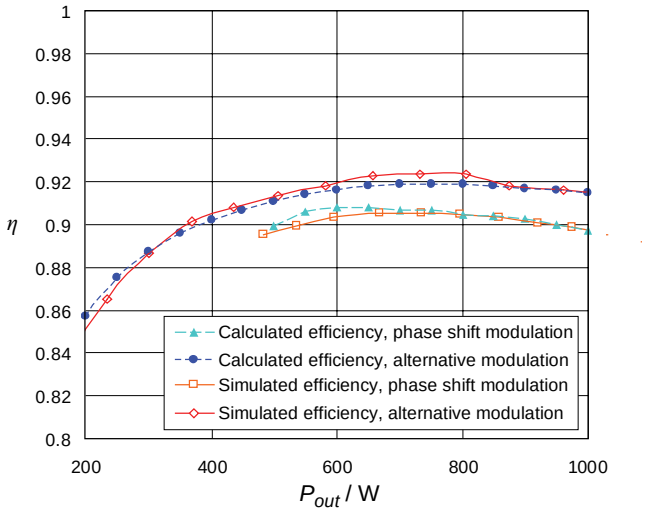


**Figure 10.** Calculated and simulated converter efficiency at nominal voltages ($V_1$ = 12 V, $V_2$ = 336 V).

measure the input and output voltages as well as the output current in order to control the output power. However, a limited soft switching range exists [2] and inefficient utilization of the converter confines the operating range to working points close to the nominal operating point.

The RMS transformer and switch currents have similar values for phase shift and the alternative modulation method at rated power. At a reduced power level, only slightly improved RMS currents are achieved for the trapezoidal and triangular modulation, so similar conduction losses can be expected.

In contrast to the conduction losses, a notable reduction in switching losses is achieved with the proposed modulation scheme. For phase shift operation 8 transistors are involved in current switching during one switching cycle leading to a comparable high level of switching losses (**Figure 9 (a)**). For the triangular modulation only two transistors need to switch current, while four transistors are involved in current switching for the trapezoidal current mode modulation during one switching period. The other transistors are operated with (or at least close to) ZCS where only small switching losses occur. This results in a significant loss reduction (Figure 9 (d)).

TABLE I
PHASE SHIFT VS. ADVANCED MODULATION

| | Phase shift modulation | Alternative modulation |
|---|---|---|
| RMS currents | Larger | Slightly smaller |
| Switching losses | Significantly higher.<br><br>8 transistors involved in current switching (during one switching cycle) | Significantly smaller.<br><br>Trapezoidal:<br>4 transistors: ZVS<br>4 transistors: ZCS<br><br>Triangular:<br>2 transistors: ZVS<br>6 transistors: ZCS |
| Converter Inductance $L$ | Larger | Smaller |
| Computation complexity | Low | CPU intensive |

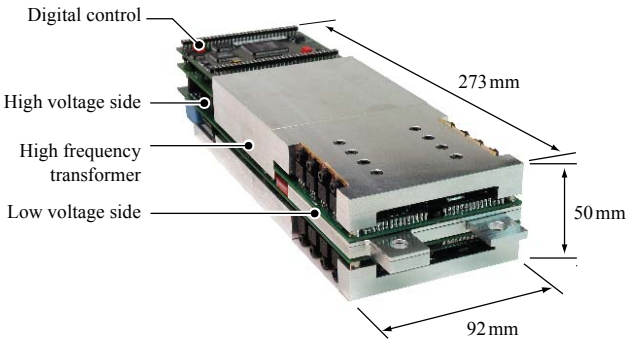


**Figure 11.** Experimental setup of the DAB

In Figures 9 (b), (c), (e), and (f) the estimated converter efficiencies are presented for different power levels and the different modulation schemes. The calculation includes MOSFET conduction and switching losses, the transformer copper and core losses, conduction losses of contact resistance on the low voltage side, and the power needed for the gate drivers. For the direction of power flow, a transfer from the low voltage side to the high voltage side is assumed. When the ratio of input and output voltages is close to the transformer turns ratio, $V_2/V_1 \approx n$, then only little improvement is achieved with the proposed modulation. For $V_2/V_1 \ll n$ or $V_2/V_1 \gg n$, improved converter utilization is achieved with the trapezoidal and triangular modulation methods. This is mainly because of the reduced amount of switching losses, but also because of smaller RMS currents. **Table I** highlights the most important differences between phase shift modulation and the alternative modulation: in order to improve the converter efficiency, more CPU intensive calculations need to be performed. A slightly reduced converter volume may be achieved because of a smaller converter inductance $L$. An efficiency gain of approximately 2% is obtained from calculations and simulation when the converter is operated with nominal input and output voltages (**Figure 10**, $V_1$=12V, $V_2$=336V).

## IV. EXPERIMENTAL VERIFICATION

The low voltage side switches of the experimental setup (**Figure 11**) are formed by four parallel-connected IRF2804 MOSFETs, and SPW47N60CFD MOSFETs are used for the high voltage side switches. The transformer is hidden under the heat sink in Figure 11, and consists of a planar core (ELP64 from EPCOS) with a single winding on the low voltage side and 24 turns on the high voltage side. A four layer PCB with 200µm copper on each layer is used to provide low losses due to the high currents on the low voltage side.

A digital signal processor is used to control the output power of the system while the modulation is implemented in a programmable logic device. For the control algorithm, a slow variation of input and output voltages is assumed, thus the amount of transferred power is defined by the current $i_L$. Therefore the DSP calculates the parameters for the modulation algorithm in order to achieve the desired power transfer. Moreover, the transformer current $i_L$ is zero at the

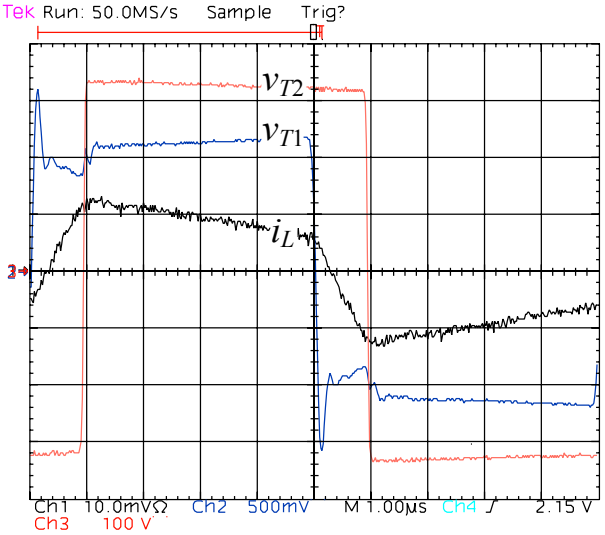


**Figure 12.** Experimental waveforms for transformer current (black) and voltages (blue: $v_{T1}$, red: $v_{T2}$) for phase shift operation, $V_1$ = 12V, $V_2$ = 336V, output power: 1kW; time scale: 1µs/Div., voltage scales: blue: 5V/Div, red: 100V/Div., current scale: 5A/Div.

end of each half cycle of the triangular and the trapezoidal modulation methods. With this approach, the converter reacts instantaneously apart from the time delay of half a switching cycle. In a first approximation, the converter can be modelled with a gain $K$.

The measured waveforms for phase shift operation are presented in **Figure 12** for $V_1$ = 12V, $V_2$ = 336V, and an output power of 1kW. For this operating point a phase angle of 29° is calculated with (2), however due to converter losses a higher phase angle of 32° is required. **Figure 13** shows the triangular modulation for an output power of 1kW at $V_1$ = 12V, $V_2$ = 400V. It can be observed that switching on the low voltage side always occurs close to zero current, and one of the bridge legs of the high voltage side is operated close to zero current. The other bridge leg is operated with ZVS with a switch current of approximately 8A. For trapezoidal modulation in **Figure 14** the operating point is $V_1$ = 12V, $V_2$ = 250V at an output power of 1kW. Combined ZCS and ZVS occur on both the low voltage and high voltage sides. The experimental waveforms show good agreement with the simulated waveforms in Figures 5 to 7.

The voltage peak that is observed during the switching of the low voltage side under current is due to the parasitic switch inductances (Figure 13, Figure 14) and causes a considerable amount of losses. Low switching losses can be achieved for the triangular current mode modulation (Figure 13) because the low voltage side switches are operated with ZCS. The highest amount of switching loss occurs for phase shift modulation because all the transistors have to switch a non-zero transformer current.

## V. CONCLUSION

In this paper the influence of phase shift modulation on the DAB's performance is investigated for high current operation. The use of alternative modulation methods is proposed in order to achieve a better performance of the converter.

It has been shown that standard phase shift modulation leads to inefficient utilization of the converter. This confines the operating range close to the nominal operating point. The converter performance can be improved with the combination of two alternative modulation schemes, the trapezoidal and the triangular current mode modulation. Despite the drawback of a higher computational effort compared to the phase shift modulation, a reduction of conduction and switching losses is achieved. This results in a significant improvement in efficiency over the full power and input and output voltage ranges.

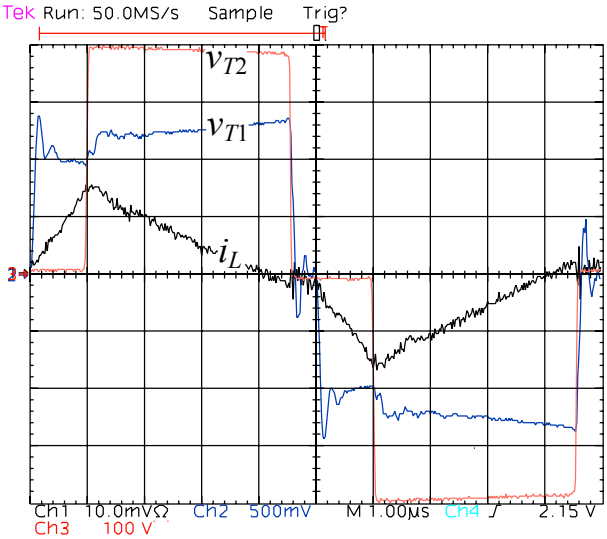


**Figure 13.** Experimental waveforms for converter current and voltages with triangular transformer current, $V_1$ = 12V, $V_2$ = 400V and an output power of 1kW; time scale: 1µs/Div., voltage scales: blue: 5V/Div, red: 100V/Div., current scale: 5A/Div.

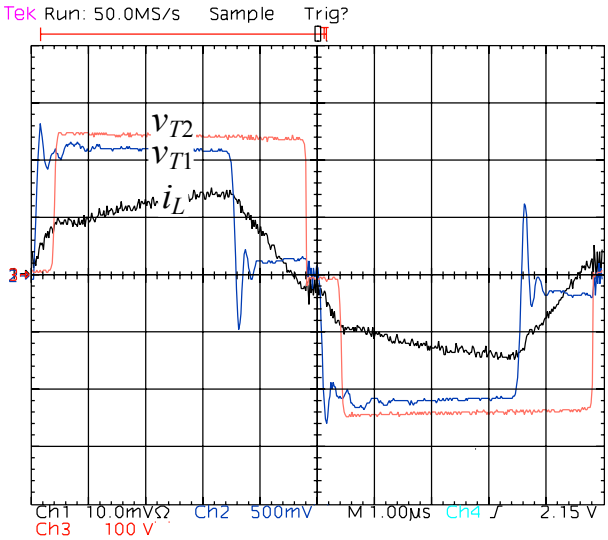


**Figure 14.** Experimental waveforms for converter current and voltages with trapezoidal transformer current, $V_1$ = 12V, $V_2$ = 250V and an output power of 1kW; time scale: 1µs/Div., voltage scales: blue: 5V/Div, red: 100V/Div., current scale: 5A/Div.

## REFERENCES


[1] Gui-Jia Su, F. Z. Peng, D. J. Adams, "Experimental evaluation of a soft-switching DC/DC converter for fuel cell vehicle applications", Power Electronics in Transportation, pp. 39-44, Oct. 2002.

[2] M. H. Kheraluwala, R. W. Gascoigne, D.M. Divan, E. D. Baumann, "Performance characterization of a high-power dual active bridge dc-to-dc converter", IEEE Transactions on Industry Applications, vol. 28, no. 6, pp. 1294–1300, Nov./Dec. 1992.

[3] J. Walter, R. W. De Doncker, "High-power galvanically isolated DC/DC converter topology for future automobiles", IEEE 34th Annual Power Electronics Specialists Conference, vol. 1, pp. 27–32, June 2003.

[4] L. Zhu, X. Xu, F. Flett, "A 3kW isolated bi-directional DC/DC converter for fuel cell electric vehicle application", Proceedings of power electronics, pp. 77–82, June 2001.

[5] N. Schibli, "Symmetrical multilevel converters with two quadrant DC-DC feeding", EPFL, Thèse Nr. 2220, pp. 99–171, 2000.

[6] D. A. Grant, J. Gowar, "Power MOSFETS: theory and applications", Wiley Intersience, 1989.

[7] S. Clemente, B. R. Pelli, A. Isidori, "Understanding HEXFET switching performance", Power MOSFET Designer's Manual, International Rectifier, 1987.